

Piezoelectric hollow cylinder with thermal gradient[†]

M. Saadatfar^{1,*} and A. S. Razavi²

¹*Faculty of Mechanical Engineering, University of Tehran, Tehran, Iran*

²*Faculty of Mechanical Engineering, University of Kashan, Kashan, Iran*

(Manuscript Received March 17, 2008; Revised September 19, 2008; Accepted October 9, 2008)

Abstract

The coupling nature of piezoelectric materials has acquired wide applications in electric-mechanical and electric devices. Recent advances in smart structures technology have led to a resurgence of interest in piezoelectricity, and in particular, in the solution of fundamental boundary value problems. In this paper, an analytic solution to the axisymmetric problem of a radially polarized, radially orthotropic piezoelectric hollow cylinder with thermal gradient is developed. An analytic solution to the governing equilibrium equations (a coupled system of second-order ordinary differential equations) is obtained. On application of the boundary conditions, the problem is reduced to solving a system of linear algebraic equations. The stress and potential field distributions in the cylinder are obtained numerically for two piezoceramics. It is shown that the hoop stresses in a cylinder composed of these materials can be decreased throughout the cross-section by applying an appropriate set of boundary conditions.

Keywords: Piezoelectric hollow cylinder; Thermal gradient; Electric potential; Radial stress; Hoop stress

1. Introduction

The development of distributed piezoelectric sensors and actuators is essential for the design of future light-weight and high-performance structures with adaptive capabilities. In addition, various piezoelectric materials have been used in many transducer designs, sonar applications, medical ultrasonic equipment, robot tactile sensors, acoustic pick-ups, force and strain gages, etc. The advance in piezoelectric materials technology has a significant impact in diverse fields, such as the space and aircraft industries. The coupling nature of piezoelectric materials has acquired wide applications in electric-mechanical and electric devices, including electric-mechanical actuators, sensors and structures. The understanding of mechanical behaviors of piezoelectric structures is thus of significant importance. Piezoelectric ma-

terials show linearity between components of stress and strain, as well as between electric field and electric displacements, only over limited ranges of mechanical or electrical applied fields. The limits of linear behavior depend on the coercive field used to polarize the material and on material composition. In recent years, there has been an accelerated effort and notable contributions in the study of thermo-electro-elastic coupling behavior in some engineering areas, including aerospace, offshore and submarine structures, chemical vessel and civil engineering structures.

Because of the difficulty related to the particular coupling effect between electric field and mechanical deformation, few problems were considered before 1990. Problems of radially polarized piezoelectric bodies were considered and solved analytically [1, 2]. In the literature the solution for isotropic medium provided static behavior such as stress concentration [2]. In [3], the static solution of radial deformation of a piezoelectric spherical shell under uniform pressures on the internal and exter-

[†] This paper was recommended for publication in revised form by Associate Editor Jeong Sam Han

* Corresponding author. Tel.: +989127476512

E-mail address: msaadatfar@ut.ac.ir

© KSME & Springer 2009

nal surfaces, and subjected to a given voltage difference between these surface, coupled with a radial distribution of temperature was successfully solved. In [4], the static solution of radial deformation of a piezoelectric cylindrical shell under uniform pressures on the internal and external surfaces, and subjected to a given voltage difference between these surface, was successfully solved.

The transient thermal stresses in a homogeneous transversely isotropic finite cylinder, due to an arbitrary internal heat generation were solved in [5]. Due to a constant temperature imposed on one surface and heat convection into the medium at the other surface, the transient thermal stresses in a homogeneous hollow cylinder were obtained in [6, 7]. Thermal shock in a hollow sphere caused by rapid uniform heating was analyzed in [8].

The piezo-thermo-elastic behavior of a pyroelectric spherical shell was investigated [9]. An exact solution of functionally graded anisotropic cylinders subjected to thermal and mechanical loads for a steady-state problem was obtained [10].

In [11], it is shown that the characteristics of wave propagation in piezoelectric cylindrically laminated shells are related to the large deformation, rotary inertia and thermal environment of the piezoelectric cylindrically laminated shells. An exact solution for stress wave propagation in piezoelectric fiber-reinforced laminated composites subjected to thermal shock loading is obtained in [12]. The dynamic focusing effects of laminated composites with piezoelectric fiber and matrix layer, subjected to thermal shock of a transitory temperature change, by means of an exact analytical solution and the corresponding numerical example is presented in [13]. In [14], a theoretical method for analyzing magneto-thermoelastic responses and perturbation of the magnetic field vector in a conducting non-homogeneous thermoelastic cylinder subjected to thermal shock by use of finite Hankel integral is investigated. In [15], an analytic solution to the axisymmetric problem of a radially polarized, spherically isotropic piezoelectric hollow sphere with thermal gradient is developed

In this paper, thermo-electro-elastic equations for linear piezoelectric solids are given. These equations are specialized to cylindrical coordinates and the axisymmetric problem described above. The governing equilibrium equations in radially polarized form are shown to reduce to a coupled system of second-order ordinary differential equations for the radial dis-

placement and electric potential field. These differential equations are solved analytically, and on applying five different sets of boundary conditions an analytic solution method for boundary value problems is developed. The stress distributions in the hollow cylinder are discussed in detail for the two piezoceramics.

2. The constitutive relation and governing equation

A cylindrical coordinate system (r, θ, z) is used. For the cylindrically symmetric problem, we have $u_\theta = u_z = 0$, $u_r = u_r(r)$. For a long orthotropic piezoelectric hollow cylinder the constitutive relations are expressed as [16]

$$\sigma_{rr} = c_{11} \frac{du_r}{dr} + c_{12} \frac{u_r}{r} + e_{11} \frac{d\psi}{dr} - \lambda_1 T(r) \quad (1a)$$

$$\sigma_{\theta\theta} = c_{12} \frac{du_r}{dr} + c_{22} \frac{u_r}{r} + e_{12} \frac{d\psi}{dr} - \lambda_2 T(r) \quad (1b)$$

$$D_{rr} = e_{11} \frac{du_r}{dr} + e_{12} \frac{u_r}{r} - \beta_{11} \frac{d\psi}{dr} + p_{11} T(r) \quad (1c)$$

$$\lambda_1 = c_{11}\alpha_1 + c_{12}\alpha_2 + c_{13}\alpha_3, \quad (1d)$$

$$\lambda_2 = c_{12}\alpha_1 + c_{22}\alpha_2 + c_{23}\alpha_3,$$

$$\lambda_3 = c_{13}\alpha_1 + c_{23}\alpha_2 + c_{33}\alpha_3$$

where c_{ij} , e_{ij} , a_i , b_{ij} , and p_{11} are elastic constants, piezoelectric constants, thermal expansion coefficients, dielectric constants, and piezoelectric coefficients, respectively. σ_{ii} and D_{rr} are the component of stress and radial electric displacement, respectively.

The equation of equilibrium is expressed as

$$\frac{d\sigma_{rr}}{dr} + \frac{\sigma_{rr} - \sigma_{\theta\theta}}{r} = 0 \quad (2)$$

In absence of free charge density, the charge equation of electrostatics is

$$\frac{dD_{rr}(r)}{dr} + \frac{D_{rr}(r)}{r} = 0 \quad (3)$$

In order to simplify calculation, the following non-dimensional forms are introduced:

$$c_i = \frac{c_{i2}}{c_{11}} \quad (i = 1, 2), \quad e_i = \frac{e_{1i}}{\sqrt{c_{11}\beta_{11}}} \quad (i = 1, 2),$$

$$D_r = \frac{D_{rr}}{\sqrt{c_{11}\beta_{11}}}, \quad \sigma_i = \frac{\sigma_{ii}}{c_{11}} \quad (i = r, \theta)$$

$$\phi = \sqrt{\frac{\beta_{11}}{c_{11}}} \frac{\psi}{b}, S = \frac{a}{b}, R = \frac{r}{b}, u = \frac{u_r}{b}$$

$$D_r = \frac{D_{rr}}{\sqrt{c_{11}\beta_{11}}}, T_i(R) = \frac{\lambda_i T(r)}{c_{11}} \tag{4}$$

$$T_p(R) = \frac{P_{11} T(r)}{\sqrt{c_{11}\beta_{11}}}$$

Then, Eqs. (1-3) can be rewritten

$$\sigma_r = \frac{du}{dR} + c_1 \frac{u}{R} + e_1 \frac{d\phi}{dR} - T_1(R) \tag{5a}$$

$$\sigma_\theta = c_1 \frac{du}{dR} + c_2 \frac{u}{R} + e_2 \frac{d\phi}{dR} - T_2(R) \tag{5b}$$

$$D_r = e_1 \frac{du}{dR} + e_2 \frac{u}{R} - \frac{d\phi}{dR} + T_p(R) \tag{5c}$$

$$\frac{d\sigma_r}{dR} + \frac{(\sigma_r - \sigma_\theta)}{R} = 0 \tag{6a}$$

$$\frac{dD_r(R)}{dR} + \frac{D_r}{R} = 0 \tag{6b}$$

Where, a and b are the inner and outer radii of the hollow cylinder, respectively, and T₀ is the reference temperature. From Eq. (6b), we have

$$D_r(R) = \frac{F_3}{R} \tag{7}$$

where F₃ is a constant. Substituting Eq. (7) into Eq. (5c), gives

$$\frac{d\phi}{dR} = e_1 \frac{du}{dR} + e_2 \frac{u}{R} - \frac{F_3}{R} + T_p(R) \tag{8}$$

Utilizing Eq. (8), Eqs. (5a) and (5b) may be rewritten as

$$\sigma_r = (1 + e_1^2) \frac{du}{dR} + (c_1 + e_1 e_2) \frac{u}{R} - \frac{e_1}{R} F_3 - T_{1p}(R) \tag{9a}$$

$$\sigma_\theta = (c_1 + e_1 e_2) \frac{du}{dR} + (c_2 + e_2^2) \frac{u}{R} - \frac{e_2}{R} F_3 - T_{2p}(R) \tag{9b}$$

Where

$$T_{1p}(R) = T_1(R) - e_1 T_p(R),$$

$$T_{2p}(R) = T_2(R) - e_2 T_p(R) \tag{9c}$$

Substituting Eqs. (9a, b) into Eq. (6a), the basic displacement equation of a transversely isotropic piezoelectric hollow cylinder is expressed as

$$\frac{d^2 u(R)}{dR^2} + \frac{1}{R} \frac{du(R)}{dR} - \frac{H_1^2 u(R)}{R^2} = I \frac{F_3}{R^2} + G_1(R) \tag{10a}$$

Where

$$H_1 = \sqrt{\frac{c_2 + e_2^2}{1 + e_1^2}}, \quad I = -\frac{e_2}{1 + e_1^2}, \tag{10b}$$

$$G_1(R) = \frac{1}{1 + e_1^2} \left[\frac{dT_{1p}}{dR} + \frac{1}{R} (T_{1p} - T_{2p}) \right]$$

The heat conduction equation for hollow cylinder can be written as

$$\frac{1}{R} \frac{d}{dR} \left(R \frac{dT}{dR} \right) = 0 \tag{11}$$

we have

$$T(R) = k_1 \ln(R) - k_2$$

$$k_1 = \frac{(T_a - T_b)}{\ln(S)}, \quad k_2 = T_b \tag{12}$$

The solution to Eq. (10a) can be written as

$$u = F_1 R^{H_1} + F_2 R^{-H_1} + (-LRV_1 H_1^2 (H_1^2 - 1) \ln(R) + (-L(V_2 + q_{11})R - IF_3)H_1^4 + (-L(V_2 + q_{11} - 2V_1)R + 2IF_3)H_1^2 + IF_3)/(H_1^2 (H_1^2 - 1)^2) \tag{13a}$$

Where F₁, F₂ and F₃ are constant, and

$$L = \frac{1}{1 + e_1^2}, \quad q_{1i} = \left(\frac{\lambda_1}{c_{11}} - \frac{e_1 P_{11}}{\sqrt{\beta_{11} c_{11}}} \right) K_i,$$

$$q_{2i} = \left(\frac{\lambda_2}{c_{11}} - \frac{e_2 P_{11}}{\sqrt{\beta_{11} c_{11}}} \right) K_i \quad i = 1, 2 \tag{13b}$$

$$V_1 = q_{11} - q_{21}, \quad V_2 = q_{21} - q_{22}$$

Since u (r) is known, the electrostatic potential is obtained from Eq. (8)

$$\phi = F_1 D_1 R^{H_1} + F_2 D_2 R^{-H_1} + F_3 D_3 \ln(R) + F_4 + D_4 \quad (14a)$$

Where F_4 is a constant, and

$$\begin{aligned} D_1 &= e_1 + \frac{e_2}{(H_1^2 - 1)^2} \left(H_1^3 - 2H_1 + \frac{1}{H_1} \right) \\ D_2 &= e_1 - \frac{e_2}{(H_1^2 - 1)^2} \left(H_1^3 - 2H_1 + \frac{1}{H_1} \right) \\ D_3 &= \frac{Ie_2}{(H_1^2 - 1)^2} \left(\frac{1}{H_1^2} - H_1^2 + 2 \right) - 1 \\ D_4 &= -[R(H_1^2 - 1)D_{41} \ln(R) + (Q_5 - Q_6)H_1^4 \\ &+ D_{42}H_1^2 + D_{43}L - Q_6 + Q_5] / (H_1^2 - 1)^2 \\ Q_5 &= \frac{k_1 p_{11}}{\sqrt{B_{11} c_{11}}}, \quad Q_6 = \frac{k_2 p_{11}}{\sqrt{B_{11} c_{11}}}, \\ D_{41} &= Q_5(1 - H_1^2) + V_1(e_2 + e_1)L \\ D_{42} &= [(V_2 - V_1 + q_{11})e_2 + e_1(q_{11} + V_2)]L \\ &- 2Q_5 + 2Q_6 \\ D_{43} &= (3V_1 - V_2 - q_{11})e_2 - e_1(-2V_1 + q_{11} + V_2) \end{aligned} \quad (14b)$$

Then, Eq. (9a) can be rewritten as

$$\sigma_r = F_1 D_5 R^{(H_1-1)} + F_2 D_6 R^{(-H_1-1)} + F_3 \frac{D_7}{R} + D_8 \quad (15a)$$

Where

$$\begin{aligned} D_5 &= (c_1 + e_1 e_2) + (1 + e_1^2)H_1 \\ D_6 &= (c_1 + e_1 e_2) - (1 + e_1^2)H_1 \\ D_7 &= \frac{I(c_1 + e_1 e_2)(-H_1^4 + 2H_1^2 + 1)}{H_1^2(H_1^2 - 1)^2} - e_1 \\ D_8 &= -[L(1 + e_1^2)V_1(H_1^2 - 1)\ln(R) \\ &+ (V_2 + q_{11} + V_1)H_1^2 - V_2 - q_{11} + V_1] \\ &- L(c_1 + e_1 e_2)V_1(H_1^2 - 1)\ln(R) \\ &+ (V_2 + q_{11})H_1^2 - V_2 - q_{11} + 2V_1 \\ &+ (H_1^2 - 1)^2 - q_{11} \ln(R) - q_{12} \end{aligned} \quad (15b)$$

Then, Eq. (9b) can be rewritten as

$$\sigma_\theta = F_1 D_9 R^{(H_1-1)} + F_2 D_{10} R^{(-H_1-1)} + F_3 \frac{D_{11}}{R} + D_{12} \quad (16a)$$

Where

$$\begin{aligned} D_9 &= (c_2 + e_2^2) + H_1(c_1 + e_1 e_2) \\ D_{10} &= (c_2 + e_2^2) - H_1(c_1 + e_1 e_2) \\ D_{11} &= \frac{I(c_2 + e_2^2)(-H_1^4 + 2H_1^2 + 1)}{H_1^2(H_1^2 - 1)^2} - e_2 \\ D_{12} &= -L(c_1 + e_1 e_2)[V_1(H_1^2 - 1)\ln(R) \\ &+ (V_2 + q_{11} + V_1)H_1^2 - V_2 - q_{11} + V_1] \\ &+ (H_1^2 - 1)^2 - L(c_2 + e_2^2)V_1(H_1^2 - 1)\ln R \\ &+ (V_2 + q_{11})H_1^2 - V_2 - q_{11} + 2V_1 \\ &+ (H_1^2 - 1)^2 - q_{21} \ln(R) - q_{22} \end{aligned} \quad (16b)$$

Five sets of boundary conditions, henceforth referred to as cases 1, 2, 3, 4 and 5, are examined.

In case 1, the cylinder is subjected to an internal uniform pressure and zero electric potential difference across the cylindrical annulus.

In case 2, free mechanical boundary conditions on both internal and external surfaces were imposed. However, there is a uniform potential difference prescribed across the annulus. For convenience, it is assumed that outer surface potential is zero, and the potential on the inner surface is a nonzero constant.

In case 3, free mechanical boundary conditions on both internal and external surfaces were imposed. However, there is a uniform potential difference prescribed across the annulus. For convenience, it is assumed that inner surface potential is zero, and the potential on the outer surface is a nonzero constant.

Case 4 is a combined loading case, i.e., a superposition of cases 1 and 3. In this case, the cylinder is subjected to an internal uniform pressure and a uniform potential difference prescribed across the annulus.

Finally, Case 5 is a combined loading case, i.e., a superposition of cases 1 and 2.

For simplicity the boundary conditions are normalized as $P_i=1$ and $\phi = 1$; therefore, the boundary conditions for each case can be written as follows:

$$\begin{aligned} \text{case1: } & \sigma_r(S) = -1, \sigma_r(1) = 0, \phi(S) = 0, \phi(1) = 0 \\ \text{case2: } & \sigma_r(S) = 0, \sigma_r(1) = 0, \phi(S) = 1, \phi(1) = 0 \\ \text{case3: } & \sigma_r(S) = 0, \sigma_r(1) = 0, \phi(S) = 0, \phi(1) = 1 \\ \text{case4: } & \sigma_r(S) = -1, \sigma_r(1) = 0, \phi(S) = 0, \phi(1) = 1 \\ \text{case5: } & \sigma_r(S) = -1, \sigma_{rr}(1) = 0, \phi(S) = 1, \phi(1) = 0 \end{aligned} \quad (17a)$$

For each of these cases, the system of linear algebraic equations for the constants F_1, F_2, A_1 and A_2 can be solved.

3. Numerical result and discussion

The numerical results are drawn in diagrams showing the variation of stress and potential across the thickness of the hollow cylinder. Mechanical, electrical and thermal properties of piezoelectric materials are listed in Table 1 [17].

The plots in the figures depict results for each of the boundary conditions, with different aspect ratio, $S= 0.25, 0.5, 0.75$. The plots in the figures depict results for $T_a=0$ and $T_b=100$. All quantities are plotted versus dimensionless radius $R=r/b$. In Figs. 1, 2, 3, 4 and 5, BaTiO₃ is shown by solid line and PZT_4 by a dashed red line.

In Fig. 1, results are shown for case 1 where internal pressure is applied. The hoop stresses in PZT_4 and BaTiO₃ experience a change of sign. In PZT_4 for $S=0.8$, most of the cylindrical cross-section is in circumferential compression (inner), and the rest (outer) is in tension. In BaTiO₃ for $S=0.25$ and 0.5 , most of the cylindrical cross-section is in circumferential compression (outer), and the rest (inner) is in tension. The change in sign is an unusual phenomenon. So far as the authors know, this does not occur in purely mechanical cylindrically orthotropic problems.

Table 1. Elastic and piezoelectric constants.

Material constant	BaTiO ₃	PZT_4
c_{11} (GPa)	150	139
c_{12} (GPa)	66	77.8
c_{13} (GPa)	66	74.3
c_{23} (GPa)	66	74.3
c_{33} (GPa)	146	115
c_{22} (GPa)	150	139
e_{11} (C/m ²)	-4.35	-5.2
e_{12} (C/m ²)	-4.35	-5.2
e_{13} (C/m ²)	17.5	15.1
β_{11} ($\times 10^{-9}$ F/m)	4.98	3.87
P_{11} ($\times 10^{-5}$ C/m ² K)	-2.0	-2.5
α_1 ($\times 10^{-5}$ 1/k)	2	2
α_2 ($\times 10^{-6}$ 1/k)	1	2
α_3 ($\times 10^{-6}$ 1/k)	1	2

The third diagram in Fig.1 shows the resulting induced electrical effect. Although the boundary conditions for case 1 require that the electric potential be zero at the inner and outer radii, an electric potential has developed in the interior of the cross-section.

Fig. 2 shows the results of case 2 (purely electrical) boundary conditions. The impressive radial stresses are interestingly minimum in the interior surface. As the S decreases to 0.6, the minimum radial stress shifts to the inner radius. The PZT_4 has greater radial stresses than BaTiO₃. The compressive hoop stress decreases from the inner to the outer radius. The BaTiO₃ has greater compressive hoop stresses than PZT_4. It can be seen that ϕ varies almost linearly between its two prescribed values.

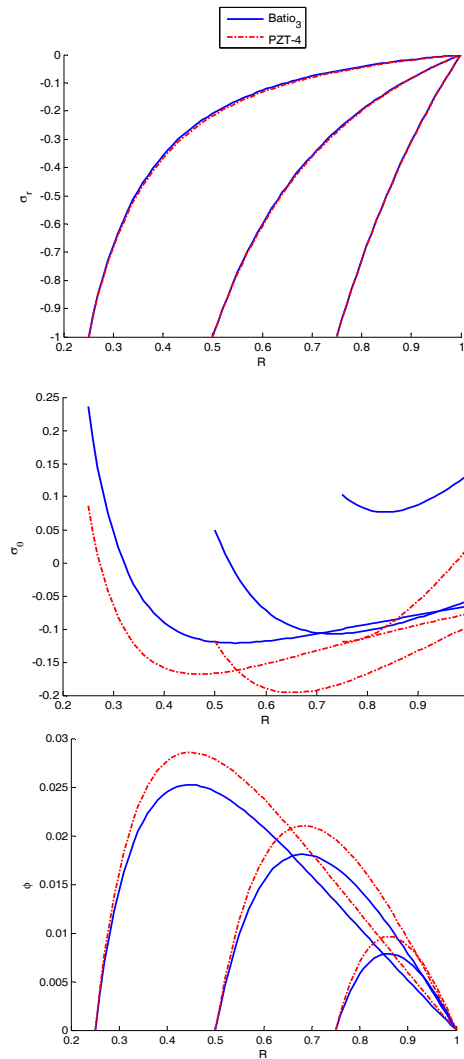


Fig. 1. Plots for stresses and potential for case 1.

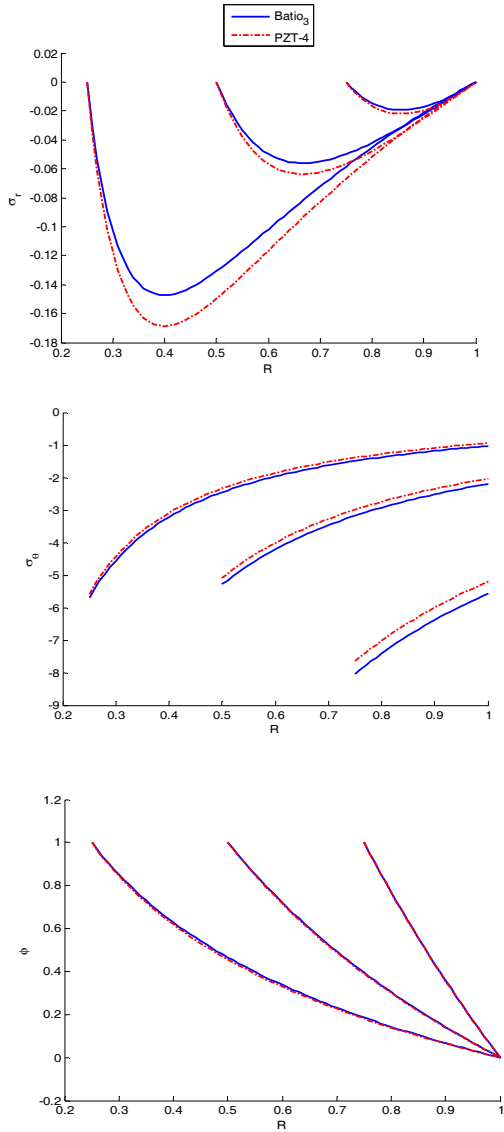


Fig. 2. Plots for stresses and potential for case 2.

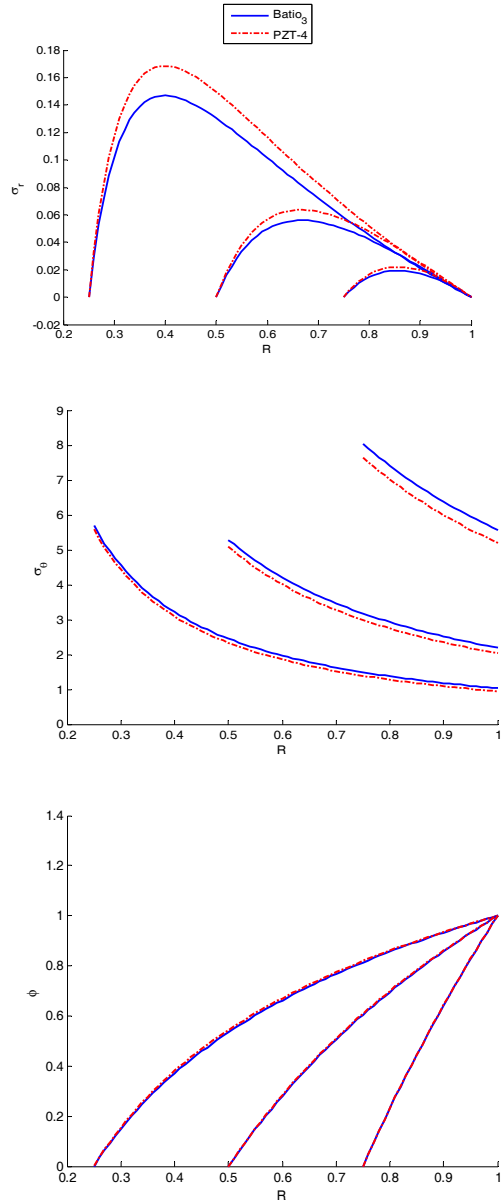


Fig. 3. Plots for stresses and potential for case 3.

Fig. 3 shows the results of case 3. Stress in this case changes with changing electric potential field direction in comparison with the previous case. The tensile radial stresses are interestingly maximum in the interior surface. The piezoceramic PZT_4 has greater stresses than BaTiO₃. The tensile hoop stress decreases from the inner to the outer radius. The magnitude of tensile hoop stress increases with increasing S.

Case 4, for which the results are shown in Fig. 4, is a superposition of cases 1 and 3, i.e., a superposition of Figs. 1 and 3. The tensile hoop stress decreases from the inner to the outer radius. The magnitude of

tensile hoop stress increases with increasing S.

Case 5, for which the results are shown in Fig. 5, is a superposition of cases 1 and 2, i.e., a superposition of Figs. 1 and 2. The compressive hoop stress decreases from the inner to the outer radius. There is very little variation between the two materials.

As is obvious from the equations for stresses and potential field, the effect of thermal constant (β_{11} , P_{11} and α_i) is slight compared with the mechanical constant (c_{ii}) in the equations.

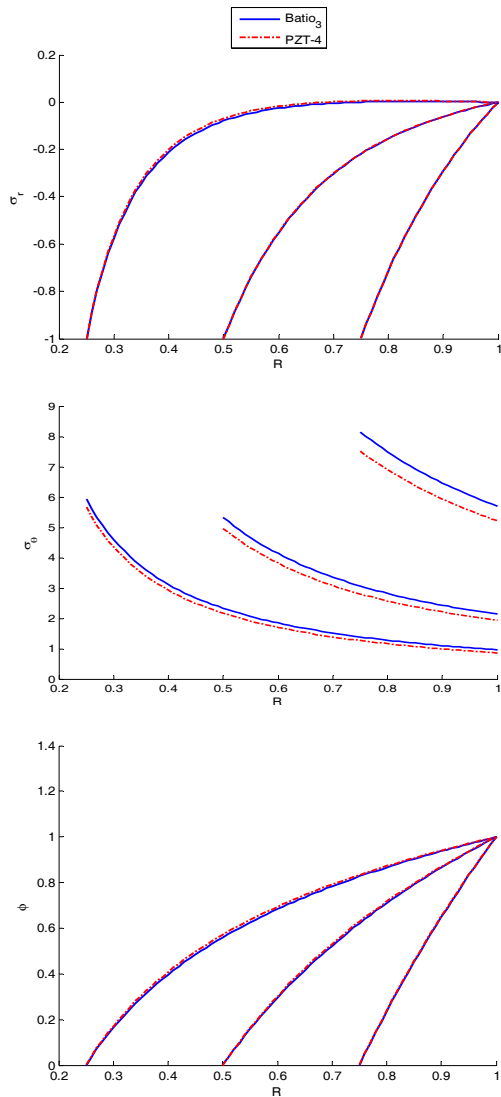


Fig. 4. Plots for stresses and potential for case 4.

As we know, changing the temperature difference between the sides of cylinder is not effective significantly on the stresses in comparison with pressure and electric potential difference. But in high change in temperature gradient (difference) some slight changes are being observed in stresses when the temperature difference is changed more than 1000°C. For example the following figure depicts the changes in radial stress for the second case of boundary condition when the temperature difference between the sides of cylinder is 100, 2000, 4000 (S=0.25).

As can be seen, there is not any significant change in PZT-4 and the changes in BaTiO₃ are slight and ignorable.

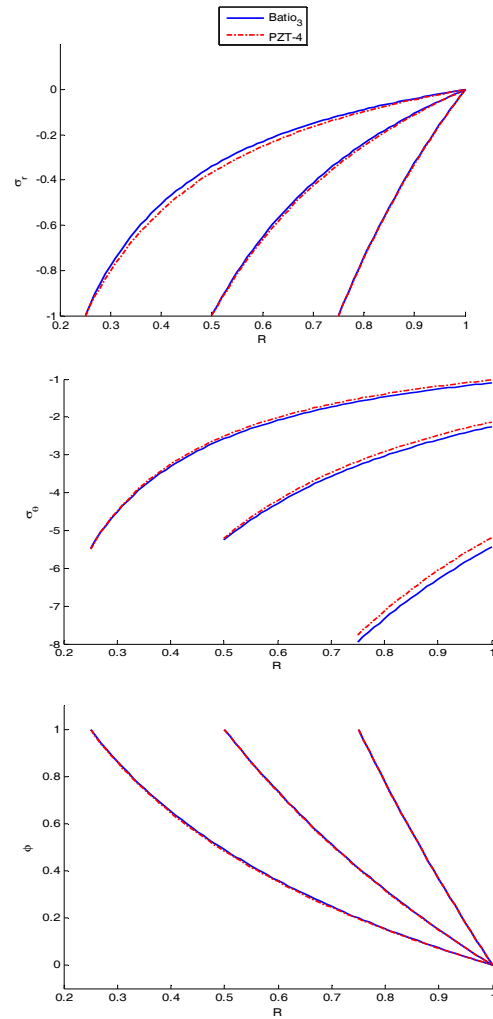


Fig. 5. Plots for stresses and potential for case 5.

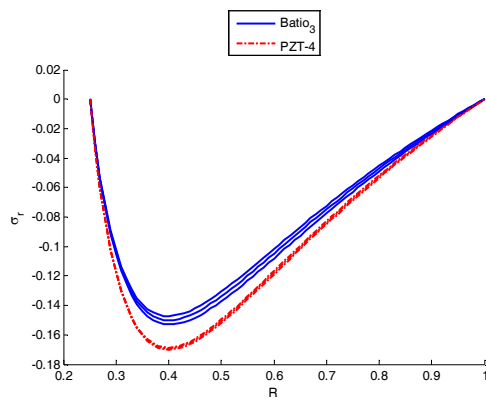


Fig. 6. Effect of change in the temperature difference.

4. Conclusion

In this research the static behavior of radially polarized piezoelectric hollow cylinder was studied and the following conclusions were reached:

In geometrically symmetric shapes, e.g., a piezoelectric cylinder that can be polarized in radial direction, mechanical and electrical effects can be investigated separately. The analysis approach presented in this research can be applied on all radially polarized piezoelectric cylinders.

A solution to the problem of static radial displacement and potential field of a piezoelectric hollow cylinder with thermal gradient, polarized in the radial direction for five different sets of boundary conditions was obtained.

Dimensionless stress distributions and electric potential curves were drawn and discussed in detail for two piezoceramics.

The technological implications of this study are significant, e.g., the amount of hoop stress resulting from mechanical loads in a hollow piezoelectric cylinder can be reduced by a suitably applied electrical field.

References

- [1] W. Q. Chen, Problems of radially polarized piezoelectric bodies, *International Journal of Solids and Structures* 25 (1999) 3206-3221
- [2] A. Ghorbanpour and S. Golabi and M. Saadatfar, Stress and Electric Potential Fields in Piezoelectric Smart spheres, *Journal of Mechanical Science and Technology* 20 (11) (2006) 1920-1933.
- [3] D. K. Sinha, Note on the radial deformation of a piezoelectric, polarized spherical shell with a symmetrical distribution, *J. Acoust. Soc. Am* 34 (1962) 1073-1075.
- [4] D. Galic and C. O. Horgan, Internally Pressurized Radially Polarized Piezoelectric Cylinders, *Journal of Elasticity* 66 (2002) 257-272.
- [5] Y. Sugano, Transient thermal stresses in a transversely isotropic finite circular cylinder due to an arbitrary internal heat generation, *Int. J. Eng. Sci.* 17 (1979) 927-939.
- [6] G. A. Kardomateas, Transient thermal stresses in cylindrically orthotropic composite tubes, *J. Appl. Mech.* 56 (1989) 411-417.
- [7] G. A. Kardomateas, The initial phase of transient thermal stresses due to general boundary thermal loads in orthotropic hollow cylinders, *J. Appl. Mech.* 57 (1990) 719-724.
- [8] T. Hata, Thermal shock in a hollow sphere caused by rapid uniform heating, *ASME J. Appl. Mech.* 58 (1991) 64-69.
- [9] W. Q. Chen and T. Shioya, Piezothermoelastic behavior of a pyroelectric spherical shell, *J. Thermal Stress* 24 (2001) 105-120.
- [10] J. Q. Tarn, Exact solutions for functionally graded anisotropic cylinders subjected to thermal and mechanical loads, *Int. J. Solids Structure* 38 (2001) 8189-8206.
- [11] X. Wang and K. Dong, Influences of large deformation and rotary inertia on wave propagation in piezoelectric cylindrically laminated shells in thermal environment, *International Journal of Solids and Structures* 43 (2006) 1710-1726
- [12] X. Wang and H. L. DAI, Stress wave propagation in piezoelectric fiber reinforced laminated composites subjected to thermal shock, *Composite Structures* 74 (1) (2006) 51-62
- [13] X. Wang and H. L. DAI, Dynamic Focusing Effects of Piezoelectric Fiber-Reinforced Laminated Composites System Subjected to Thermal Shock, *Journal of Thermal Stresses* 28 (8) (2005) 817-838,
- [14] X. Wang and K. Dong, Magneto-thermodynamic stress and perturbation of magnetic field vector in a non-homogeneous thermoelastic cylinder, *European Journal of Mechanics A/Solids* 25 (2006) 98-109,
- [15] M. Saadatfar and A. Rastgoo, Stress in Piezoelectric Hollow Sphere with Thermal Gradient, *Journal of Mechanical Science and Technology*, 22 (2008) 1-8
- [16] H. L. Dai and X. Wang, Thermo-electro-elastic transient responses in piezoelectric hollow structures, *International Journal of Solids and Structures* 42 (2005) 1151-1171
- [17] H. L. Dai and X. Wang, Stress wave propagation in laminated piezoelectric spherical shells under thermal shock and electric excitation, *European Journal of Mechanics A/Solids* 24 (2005) 263-276.



Mahdi Saadatfar received a B. S. degree in Mechanical Engineering from University of Kashan 2006. He is currently a M.S student at the School of Mechanical Engineering at University of Tehran, Iran. He is currently researching about modeling of nanoindentation process in nanocomposites. Mr. Saadatfar's research interests are in the area of piezoelectric Materials, Polymer/Clay nanocomposites and Finite element modeling. He has several published paper about piezoelectric materials and Finite element modeling of nanocomposites.



Amin Shariat Razavi received a B.S degree in Mechanical Engineering from Kashan University in 2006. He is currently testing and examining an specific type of intelligent plasma cutting machine for process equipment that is designed by himself. Mr. Razavi's research interests are smart materials and design of mechanical system.